

# The Effect of Annealing Temperature and Quenching Media Variations On Heat Treatment Process of Cu-Zn-Al Shape Memory Alloys For Shape Memory Effect and Microstructure

Mavindra Ramadhani\*, Rochman Rochiem, Rizki, M. Arfani

Materials and Metallurgical Department, Faculty of Industrial Technology and System Engineering,  
Institut Teknologi Sepuluh Nopember, Surabaya

Email: mavindra@its.ac.id\*

Received: 2023-05-09 Received in revised from: 2023-05-17 Accepted: 2023-05-17

## Abstract

Shape Memory Alloys (SMA) is a material that can return to its original shape after undergoing mechanical deformation. The most commonly SMA material used is the Ni-Ti alloy. However, it is high cost. So that it is necessary to have alternative materials, for instance Cu-Zn-Al. Several studies related to Cu-Zn-Al Shape Memory Alloys have poor mechanical properties. So there further research required in order to determine the heat treatment process of Cu-Zn-Al Shape Memory Alloys. In this study Cu-21Zn-5Al alloys were given heat treatment with annealing temperature variations (425;550;600°C) and cooling media (brine, dry ice). Annealing process affects the mechanical properties and microstructure of the test material. Cooling media results the cooling rate during solution treatment. Tests in this study include hardness test, metallographic test, XRD test, DSC test, and SME test. From the test results, it was found that all the test variables have the Shape Memory Effect. The variable that had the greatest recovery (38.3%) was annealing temperature of 450°C with the cooling solution media using brine. In addition, the most rapid cooling occurs in the brine cooling media.

**Keywords:** *Cu-Zn-Al, Shape Memory Alloys, Heat Treatment, Shape Memory Effect, Microstructure*

## 1. Introduction

Shape Memory Alloys (SMA) research has been accelerated in the previous decade. This material possesses form recovery capabilities, which allow it to return to its original shape. After mechanical deformation. Currently, many materials, such as Shape Memory Alloys (SMAs), have been produced. Nickel and Titanium alloy, also known as NiTiNOL (Ni- Ti Naval Ordnance Laboratory). There are numerous alloys. It was developed because of its mechanical capabilities and form recovery properties. However, this alloy has limitations, such as complicated processing and high manufacturing costs. This piques curiosity in the search for alternate materials for Shape Memory. Other alloys include Cu-Zn-Al alloys.

In 2019, Alizadeh et al. conducted research on multilayer Cu-Zn-Al composites formed via roll bonding and then subjected to temperature fluctuations during heat treatment. According to the findings of these experiments, the higher the heat treatment temperature, the greater the increase in mechanical characteristics gained (the temperatures employed were 750°C, 825°C, and 900°C). Garias Devara investigated the effect of media fluctuations coolant in the Cu-Zn-Al Shape Memory Heat Treatment method Alloys the same year. There were difficulties encountered during the material bending procedure in this study. This is owing to the material being fairly hard, making it difficult to form.

Due to a paucity of study on shape memory alloys Cu-Zn-Al, there is presently no way for producing such alloys. When compared to NiTiNOL, ideal for improved recovery qualities. As a result, this study will look into form memory alloys Cu-Zn-Al and how annealing temperature and cooling media modifications affect shape memory effect and microstructure. After the machining process, the mechanical characteristics and microstructure of the test material are affected by the annealing procedure. The cooling medium influences the pace of cooling after solution treatment as well as the recovery properties. The selection of variables in this study was based on the influence of each of these processes. So from therefore, in this study there are several tests for strengthen the hypothesis, such as hardness testing, XRD testing, DSC testing, metallographic testing, and Shape Memory Effect test.

## 2. Method

The Cu-21Zn-5Al alloy obtained from the casting process was tested for hardness, metallography and XRD. The alloy is given heat treatment starting from homogenizing followed by metallographic testing. By preparing the specimen to be put into the furnace and heated to a temperature of 850°C for 2 hours. Then, removed from the furnace and cooled in air to room temperature. Next, the machining process and annealing process are carried out by inserting the AB and AI specimens into the furnace and heating them to 425°C for 4 hours. After that, it was cooled in air and the BB and BI specimens were put into the furnace to be heated at 550°C for 4 hours. Cooled again in air and put the CB and CI specimens into the furnace at 600°C for 4 hours. Metallographic testing was carried out. The final step is solution treatment by putting all the specimens into the furnace to be heated at 850°C for 10 minutes. Then, it is taken out to be cooled in a cooling medium in the form of brine solution for AB, BB, CB specimens and dry ice media for AI, BI, CI specimens. All specimens were tested for hardness, metallography, XRD, DSC, SME

## 3. Results and Discussion

In this research, there is Cu-21Zn-5Al alloy in Figure 1 which is result of casting. This alloy has been tested using X-Ray Fluorescence (XRF) MiniPal4 PANanalytical.

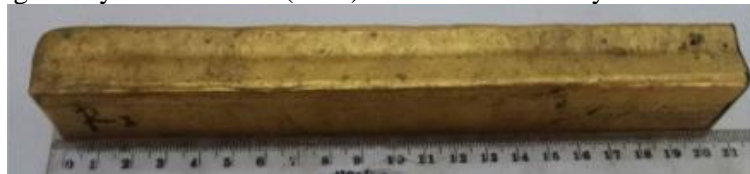


Figure 1. Cu-21Zn-5Al Alloy

The hardness test in this study was performed using a universal hardness tester HBRV 187.5 A and specimens tested as cast specimens, with specimens from each variable carried out for the heat treatment process. The test specimen is subjected to a 30 kgf load with a 10-second indentation duration. Each specimen was examined three times, and an average value was calculated, resulting in data indicating that the hardness value was as indicated in Figure 2. Because to nucleation during the casting process, phase  $\alpha$  was produced in the as cast specimens, resulting in a low hardness value. Meanwhile, the homogenizing specimen has a somewhat lower hardness value due to the formation of more phases. The annealing results yielded further specimens. The hardness value is said to decrease as the annealing temperature rises. The specimens with brine cooling media have the highest hardness value when examined from the cooling medium because the martensite phase developed is relatively dominating compared to the  $\alpha$  phase. Because the dominant  $\alpha$  phase is generated, it gives nearly the same hardness value as the as cast specimen for dry ice cooling media. It may be determined that the AB specimen has the highest hardness value, making it resistant to plastic deformation.

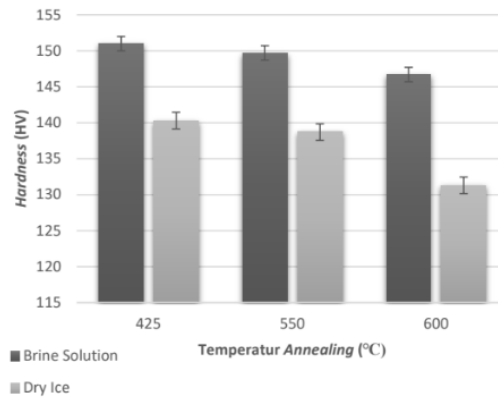


Figure 2. Graph of Result Hardness Test

Metallographic testing using Metallurgical Microscope OLYMPUS BX51M-RF. The specimens used were square in shape with dimensions of 2.5 cm x 2 cm x 1 cm. The etching solution used was 5 grams of FeCl<sub>3</sub>, 100 ml of ethanol, and 10 ml of HCl with the immerse method for 10-20 seconds. Table 1 shows the percentage of phases present in the specimens analyzed using the FIJI.App.

Tabel 1. Analyze Result of Percentage Phases

| Spesimen     | % Area   |         |          |           |
|--------------|----------|---------|----------|-----------|
|              | $\alpha$ | $\beta$ | $\gamma$ | Martensit |
| As Cast      | 65       | 31,3    | 3,7      | -         |
| Homogenizing | 70       | 28,5    | 1,5      | -         |
| Machining    | 47,3     | 30      | 2        | 20,7      |
| Anneal 425°C | 60,8     | 15,2    | 2,5      | 21,5      |
| Anneal 550°C | 63       | 17,5    | 2        | 17,5      |
| Anneal 600°C | 64,8     | 18,3    | 1,3      | 15,6      |
| AB           | 25,8     | 5,4     | 7        | 61,8      |
| BB           | 27,3     | 7,4     | 6        | 59,3      |
| CB           | 30,4     | 8,5     | 3        | 58,1      |
| AI           | 50,3     | 20,7    | 5,6      | 23,4      |
| BI           | 53,3     | 21,5    | 5        | 20,2      |
| CI           | 55,3     | 23,3    | 4        | 17,4      |

From Figure 3, it shows if the specimen contained phase  $\alpha$  has bright colour,  $\beta$  has dark colour, and  $\gamma$  makes black point. The different colours has formed because of the phase's response of etch solution so it makes different intensity of light [5]. In Figure 4 shows if  $\alpha$  phase is the most dominant phase in specimen at 65%. Homogenizing's result of microstructure looks more homogeny than other. It can conclude from  $\alpha$  phase's size which more uniform. And then, recrystallization process of  $\alpha$  phase makes the  $\beta$  and  $\gamma$  phases is less. Figure 5 demonstrates that the form of each phase is uneven due to grain elongation in some of the phases. This is due to uneven heat generated during the machining process. It can also be seen that martensite forms as a result of the dissolution of phase  $\alpha$  on phase  $\beta$ . Furthermore, the cooling rate is uneven, causing some of them to crystallize. While Figure 6 indicates that as the annealing temperature rises, the fraction of phases  $\alpha$  and  $\beta$  increases because the material's freezing time increases, so does the crystallization time. Furthermore, the microstructure results in Figure 7 reveal that the martensite in the specimens solution treated with a cooling medium in the form of brine was significantly higher than in the others. It produces significantly more martensite at 850C because phase  $\alpha$  dissolved in  $\beta$  does not have time to crystallize in equilibrium throughout the heating process. If the dry ice cooling medium only generates rapid cooling on specific surfaces, the cooling is not dispersed evenly. This is seen in Figure 8, which depicts the dominating  $\alpha$  phase.

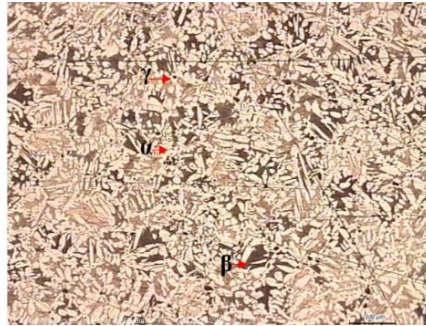


Figure 3. Microstructure of Specimen As Cast Using Magnification 100x

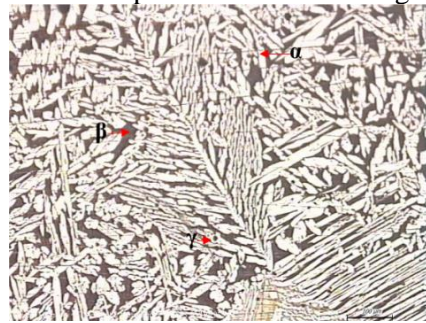


Figure 4. Microstructure of Specimen Homogenizing Using Magnification 100x

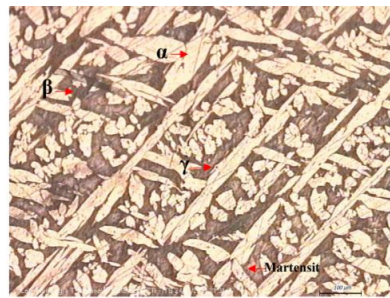


Figure 5. Microstructure of Specimen After Machining Using Magnification 100x

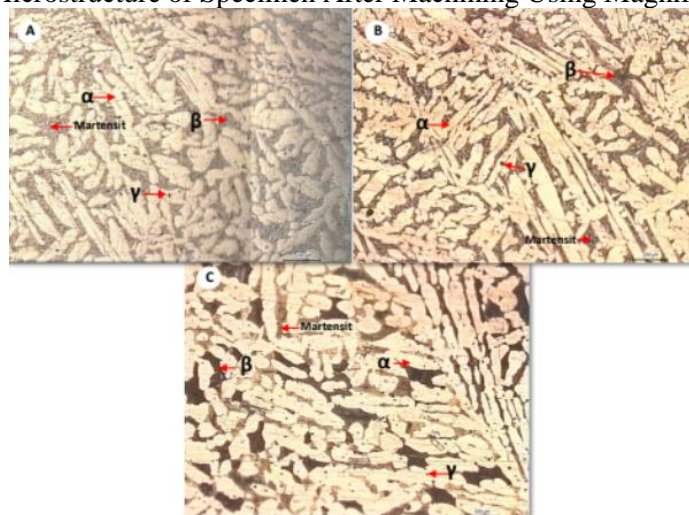


Figure 6. Microstructure of Specimen After Annealing at Temperature (A) 425°C; (B) 550°C, (C) 600°C Using Magnification 100x



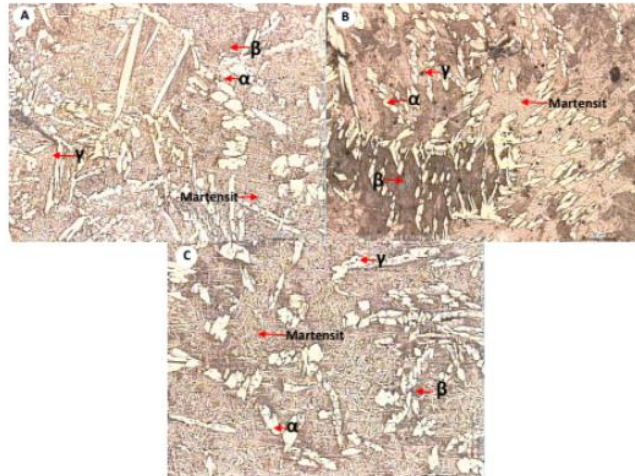


Figure 7. Microstructure of Specimen (A) AB; (B) BB, (C) CB Using Magnification 100x

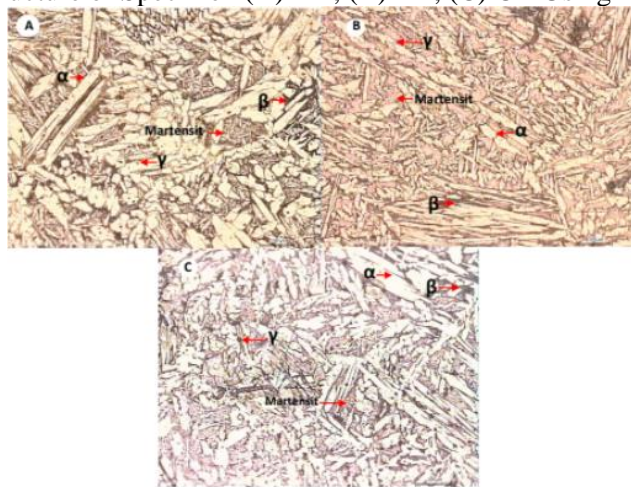


Figure 8. Microstructure of Specimen (A) AI; (B) BI, (C) CI Using Magnification 100x

The XRD test is used to detect the phase transition created on the specimen, and the results are compared with International Center of Diffraction Data (ICDD) standard data using the High Score Plus-Marven PAN Analytical program. Figure 9(A) depicts the results of the XRD test. One of the phases generated is  $\alpha$ -brass, which has a cubic crystal structure and may be found in all specimens of varying strengths. The peak position in the as cast specimen is  $2\theta$  42.325 in field (1,1,1),  $2\theta$  49.275 in field (2,0,0), and  $2\theta$  87.454 in field (3,1,1). Furthermore,  $\beta$ -brass phase is visible at the peak positions  $2\theta$  42.612 in field (1,1,1) and  $2\theta$  72.675 and 88.898 in field (3,1,1). For the  $\gamma$ -brass phase at position  $2\theta$  43.311 in plane (3,3,0) and position  $2\theta$  79.456 in plane (6,3,3). In Figure 9(A), it can conclude that intensity of phase  $\alpha$ -brass bigger than intensity of specimen as cast but for phase  $\beta$ -brass lower. Because of quenching makes the phase  $\alpha$  dissolve into phase  $\beta$  and become martensite at room temperature. In Figure 9(B), dry ice affects slow rapid cooling for specimen so phase  $\alpha$  have much time to dissolve into phase  $\beta$  and recrystallization.

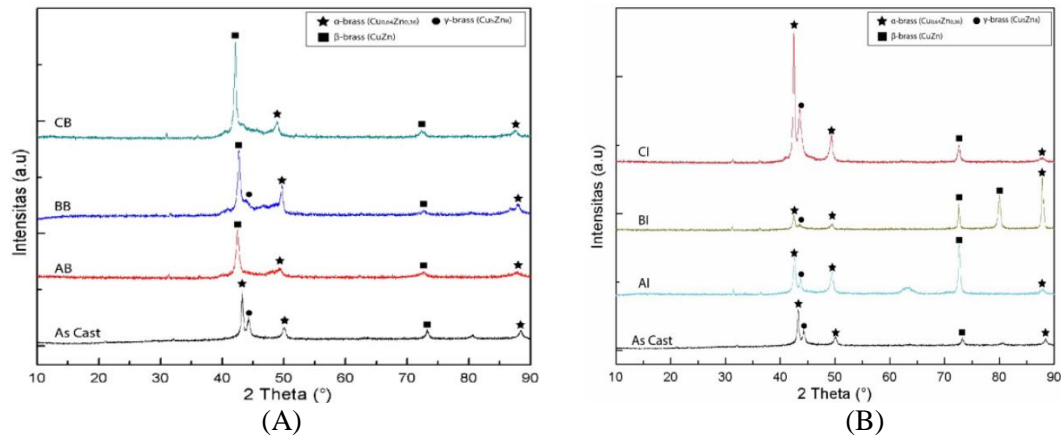


Figure 9. XRD's Result of Specimen in Cooling Media (A) Brine (B) Dry Ice

The DSC test is used to determine the phase transition of the specimen at a heating rate of 10°C per minute and a temperature range of 25 to 400°C. Shape Recall Alloys have four transition temperatures from low to high temperatures: Martensite Finish ( $M_f$ ), Martensite Start ( $M_s$ ), Austenite Start ( $A_s$ ), and Austenite Finish ( $A_f$ ) [24]. The exothermic peak is defined by a decrease in heat flow around 152.9°C in the midway of  $M_f$  and  $M_s$ . Meanwhile, a rise in heat flow with peaks in the austenite temperature range indicates an endothermic process. Transformation temperature from DSC's result can be seen in Table 2.

Table 2. Transformation Temperature of Specimen BB

| Temperature (°C) |       |       |       |       |       |
|------------------|-------|-------|-------|-------|-------|
| $M_f$            | $M_p$ | $M_s$ | $A_s$ | $A_p$ | $A_f$ |
| 94,8             | 152,9 | 197,7 | 275,4 | 282,2 | 289,6 |

Shape Memory Effect Test based on ASTM F2082-01 using specimen in wire shape with diameter 1 mm and length 10 cm. The test begins by bending the test specimen to a 20°, as indicated in Figure 10(A). Then it is heated in a furnace to 200°C and held for 5 minutes to allow for recovery. Figure 10(B) depicts shape recovery, with percentages indicated in Table 3. When the test specimen is bent as a result of stress, the arrangement changes from twinned martensite to detwinned martensite. The heating causes detwinned martensite to be transformed into austenite [23]. Specimens with brine cooling media have a greater recovery value than dry ice based on Figure 11. This is caused by the martensite phase which affects the recovery.

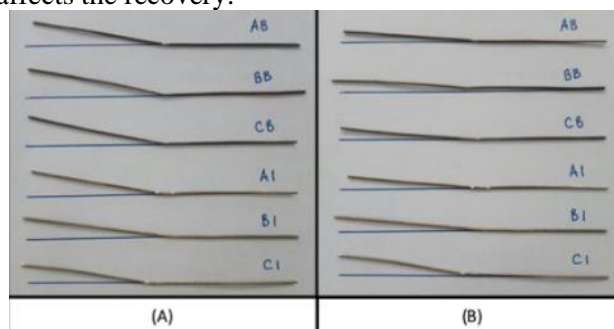


Figure 10. Specimen for Shape Memory Effect Test (A) Before Shape Recovery (B) After Shape Recovery

Table 3. Percentage of Shape Recovery Every Specimen

| No | Variable | Shape Recovery (%) |
|----|----------|--------------------|
| 1  | AB       | 38,3% ± 12,58      |
| 2  | BB       | 36,7% ± 12,58      |
| 3  | CB       | 28,3% ± 10,40      |
| 4  | AI       | 21,7% ± 7,63       |
| 5  | BI       | 16,7% ± 7,64       |
| 6  | CI       | 10% ± 5,00         |

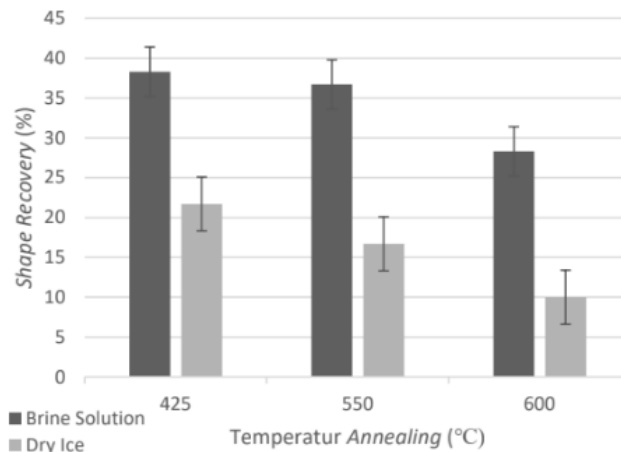


Figure 11. Bar Diagram of Shape Recovery

#### 4. Conclusion

In longer alloys, the cooling rate decreases as the annealing temperature rises. At the greatest annealing temperature of 600°C with dry ice cooling medium, the martensite phase is somewhat more prevalent, at 17.4%, and has the worst shape memory effect, with a recovery of 10%. This has an impact on the crystallization process that takes place. The martensitic phase is significantly more prevalent, at 61.8%, at the lowest annealing temperature of 425°C with brine, and the shape memory effect is strongest, with a recovery of 38.3%. The brine cooling medium solution cools down the quickest. This is due to the fact that the brine solution's liquid state accelerates the cooling process, resulting in the formation of a very big martensite with a martensite content of 61.8% and a good shape memory effect with a recovery value of 38.3%. The cooling process on specimens is uneven due to the solid form that dry ice possesses, therefore it tends to be more the dominant phase generated, which has attributes equal to 55.3%. Owned shape memory impact is only 10%, which is quite low.

#### 5. Acknowledgments

The authors would like to express their gratitude to the following individuals and organizations for their support and assistance in conducting this research, including author's parents for their love and support; Siti Nurfitriana and Siti Nurfasyilla as author's sister who always give motivation and support; Ica, Lucky, Eka, Handis as Final Assigment's partner who also help and work together; Mr. CC. Mudjianto, Mr. Sutari, Mr. Chanan who help author during final assignment; MT18's big family as author's family while studying in DTMM ITS; Antasena's team who gives experience and knowledge; author's friend in Spnsorship and Relationship Division in Antasena; HMMT FTI-ITS and especially author's friend in SOSMAS; big family of LDJ Ash-Haabul Kahfi and INDOCOR ITS SC; author's friend in house rent and author's senior. Thank you very much for the support and enthusiasm that has been given. Hopefully this research can be useful for development of technology and science.

## Referensi

- [1] \_\_\_\_\_, "ASM Handbook Volume 2 : Properties and Selection : Nonferrous Alloys and Special-Purpose Materials," *ASM International Handbook Committee*, 1990.
- [2] \_\_\_\_\_, "ASM Handbook Volume 3 : Alloy Phase Diagrams," *ASM International Handbook Committee*, 1992.
- [3] \_\_\_\_\_, "ASM Handbook Volume 4 : Heat Treating," *ASM International Handbook Committee*, 1991.
- [4] \_\_\_\_\_, "ASM Handbook Volume 8 : Mechanical Testing and Evaluation," *ASM International Handbook Committee*, 2000.
- [5] \_\_\_\_\_, "ASM Handbook Volume 9 : Metallography and Microstructures," *ASM International Handbook Committee*, 2004.
- [6] \_\_\_\_\_, "ASM Handbook Volume 10 : Materials Characterization," *ASM International Handbook Committee*, 1992.
- [7] \_\_\_\_\_, "ASM Handbook Volume 16 : Machining," *ASM International Handbook Committee*, 1995.
- [8] Adiguzel, "Smart Materials And The Influence Of Atom Sizes On Martensite Microstructures In Copper-Based Shape Memory Alloys," *Journal of Materials Processing Technology*, 2007.
- [9] Alizadeh, Morteza., and Avvazadeh, Mahsa, "Evaluation of Cu-26 Zn-5 Al Shape Memory Alloys Fabricated by Accumulative Roll Bonding Process". *Materials Science and Engineering*, vol. 757, pp. 88-94. 2019.
- [10] Arif, Saiful, "Pengaruh Parameter Proses Gerinda Permukaan Terhadap Temperatur dan Hasil Penggerindaan," Kediri: Multitek Indonesia. 2017.
- [11] Aryawan, I Putu Yudi., Wijaksana, Hendra., Suarnadwipa, I Nengah, "Study Eksperimental Performa Pendingin Ice Bunker dengan," *Jurnal Ilmiah Teknik Desain Mekanika*, vol. 5, no. 3, pp. 1-5. 2016..
- [12] ASTM F2082, "Standard Test Method for Determination of Transformation Temperature of Nickel-Titanium Shape Memor Alloys by Bend and Free Recovery," *ASM International*, pp. 1-6. 2015.
- [13] ASTM E92-17, "Standard Test Method for Vickers Hardness of Metallic Materials," *ASM International*, pp. 1-3. 1997.
- [14] ASTM F2005, "Standards for Ni-Ti Alloys," *ASM International*, pp. 2-5. 2004.
- [15] Avner, S.H, "Introduction to Physical Metallurgy," *New York: McGraw-Hill Book Company*. 1974.
- [16] Callister, William, "Material Science and Engineering an Introduction 9th Edition," *New York: John Wiley & Sons, Inc.* 2013.
- [17] Castro, M.L., Romero, R, "Isothermal  $\gamma$  Precipitation in  $\alpha \beta$  Cu-Zn-Al Alloy," *Elsevier Science S.A. A*, vol. 255, pp. 1-6. 1998.
- [18] Chen, Xinren., Zhang, Fan., Chi, Menyuan., Yang, Shuiyuan., Wang, Cuiping., Liu, Xingjun., Zheng, Songsheng, "Microstructure, superelasticity and shape memory effect by stress-induced martensite stabilization in Cu-Al-Mn-Ti shape memory alloys," *Materials Science and Engineering A*, vol. 236-237, pp. 10-17. 2018.
- [19] Cimpoesu, Ramona., Florea, Costel., Stanciu, Sergiu., Bejinariu, Costica. 2017. "Advance Shape Memory Elements for Automotive Industry". *International Journal of Modern Manufacturing Technologies*, vol. 2067, pp. 3604. 2017.
- [20] Dasgupta, Rupa, A. K. Jain, P. Kumar, S. Hussein, A. Pandey, "Effect of Alloying Constituents on the Martensitic Phase Formation in Some Cu-Based SMAs," *Journal of Materials Research and Technology*, vol. 3, pp. 264-273. 2014.
- [21] Devara, Garias, "Pengaruh Variasi Media Pendingin Pada Proses Heat Treatment Cu-21,8Zn-7Al Shape Memory Alloy Terhadap Efek Shape Memory dan Struktur Mikro," Surabaya:ITS. 2019.
- [22] Groover, M, "Fundamental of Modern Manufacture 4<sup>th</sup> Edition," *USA : John Wiley & Sons, Inc.* 2010.



- [23] Kumar, P.K. dan D. C. Lagoudas, "Shape Memory Alloys: Modelling and engineering Applications," US : Springer. 2008.
- [24] Lobo, Paulo Silvia, J. Almeida, L. Guerreiro, "Shape Memory Alloys Behaviour: A Review," *Procedia Engineering*, vol. 114, pp. 776-783. 2015.
- [25] Meng, Lifang., Zhang, Zheng., Zhang Yueling., Zhang, Jinxu., Yang, Xu., Gao, Hongliang., Shu, Baipo, "The Influence of Stacking Fault Energy on Mechanical Properties of Cu-Al-Zn Alloys Processed by Surface Mechanical Attrition Treatment," *Elsevier Science S.A*, vol. 744, pp. 235-240. 2019.
- [26] Perkins, Jeff, "Shape Memory Effect in Alloys," California: Springer Science + Business Media, LLC. 1975.
- [27] Rabbani, Raihan Abrar, "Pengaruh Variasi Media Pendingin Pada Proses Heat Treatment Cu-23,6Zn-5Al Shape Memory Alloys Terhadap Efek Shape memory dan Struktur Mikro," Surabaya: ITS. 2019.
- [28] Sargent, Philip M, "Indentation Size Effect and Strain-Hardening," *Research Gate*, vol. 744, pp. 235-240. 2015.
- [29] Surdia, Tata dan Shinroku Saito, "Pengetahuan Bahan Teknik.," Bandung: Pradnya Paramita. 1999.
- [30] Wijaya, Andreas., Nasution, Fajar H., Tjandrawinata, Rosalina., Yusra, Yohana, "Perbandingan Komposisi Unsur Piranti Retensi Nikel Titanium dengan Nikel Titanium Superelastic dan Uji Sifat Kelelahan Logam, ". ISSN (P), pp. 2460-8696. 2017.